PHYSICAL REVIEW B **89**, 020507(R) (2013)

Superconductivity in $LiFeO_2Fe_2Se_2$ with anti-PbO-type spacer layers

X. F. Lu,[1] N. Z. Wang,[1] G. H. Zhang,[2,3] X. G. Luo,[1] Z. M. Ma,[3] B. Lei,[1] F. Q. Huang,[2,3,*] and X. H. Chen[1,†]

[1]*Hefei National Laboratory for Physical Science at Microscale and Department of Physics, University of Science and Technology of China, Hefei, Anhui 230026, People's Republic of China*

[2]*CAS Key Laboratory of Materials for Energy Conversion, Shanghai Institute of Ceramics, Chinese Academy of Sciences, Shanghai 200050, China*

[3]*Beijing National Laboratory for Molecular Sciences and State Key Laboratory of Rare Earth Materials Chemistry and Applications, College of Chemistry and Molecular Engineering, Peking University, Beijing 100871, China*

(Received 9 October 2013; revised manuscript received 11 December 2013; published 22 January 2014)

We report on a superconductor $LiFeO_2Fe_2Se_2$ with $T_c \sim 43$ K, synthesized via the hydrothermal method. The anti-PbO-type spacer layer of $LiFeO_2$ has been successfully intercalated between the anti-PbO-type FeSe layer, which results in a high-T_c superconductivity in this iron selenide material. In this material, the $LiFeO_2$ layer is electrically neutral and does not act as an electron donor, which is remarkably different from other heavily electron-doped intercalated FeSe-derived superconductors. Based on our results and previous reports on FeSe-based superconductors, we figure out a V-shaped anion height from the Fe layer dependence of T_c in the FeSe-derived superconductors, which is in contrast to the inverse V-shaped one for the FeAs-based superconductors. Our studies expand the categories of the iron-based superconductors and open a door in the quest for potential superconductors with various spacer layers, which is helpful for the study of the underlying physics in iron-based high-T_c superconductors.

DOI: 10.1103/PhysRevB.89.020507 PACS number(s): 74.70.Xa, 74.10.+v, 74.62.Fj, 81.20.−n

Superconductivity has been found in iron arsenides with a great diversity of crystallographic structures by alternately stacking the conducting FeAs layers and various spacer layers, including alkali or alkali-earth metal ions and PbO- or perovskite-type oxide blocks.[1–10] A T_c as high as 55 K in FeAs-derived compounds has been achieved in the *Ln*OFeAs compounds (1111 phase, *Ln* = La, Ce, Pr, Nd, Sm, etc.) with PbO-type oxide spacer layers.[10] β-FeSe has a basic structure similar to that of the FeAs layer in iron arsenide superconductors, and shows superconductivity with $T_c \sim 8$ K.[11] However, there exists a remarkable difference between these structural elements. The $Fe^{2+}Se^{2-}$ layer is neutral, while the $Fe^{2+}As^{3-}$ layer possesses negative charges. It is the electric neutrality that makes the physical properties and structural categories of FeSe-derived compounds different from those of the FeAs-derived compounds.

In iron selenides, metal ions and molecules have been intercalated between adjacent FeSe layers as spacer layers to form superconductors with high T_c, such as $A_xFe_{2-y}Se_2$ (A = K, Rb, Cs, Tl/K and Tl/Rb, etc.), $Li_x(NH_2)_y(NH_3)_{1-y}Fe_2Se_2$, and $Li_x(C_5H_5N)_yFe_{2-z}Se_2$.[12–18] In $A_xFe_{2-y}Se_2$ single crystals, there are two distinct phases: a superconducting phase with $T_c \sim 32$ K and without Fe vacancies,[19] and an insulating antiferromagnetically ordered phase, $K_2Fe_4Se_5$, with a Néel transition temperature of ~560 K and a $\sqrt{5} \times \sqrt{5}$ order of Fe vacancies.[19,20] However, the superconducting phase can be observed only if it is in close proximity to the insulating one. It seems that the insulating phase $A_2Fe_4Se_5$ plays a crucial role in the superconductivity of $A_xFe_{2-y}Se_2$, and some indeed argue that it is probably the parent compound for this type of material.[21] Such inhomogeneity makes the investigation of the underlying physics in $A_xFe_{2-y}Se_2$ complicated. In alkali metal–molecular intercalated iron selenide superconductors, the structures of the space layers are relatively complex, and whether the space layers act as charge donors or simply as spacer units is still a puzzle.[16–18] In order to acquire a better understanding of the underlying physics in FeSe-derived and other related high-T_c superconductors, it is of significance to search for superconductivity in intercalated FeSe systems with novel spacer layers.

In this Rapid Communication, we report on an iron selenide superconductor $LiFeO_2Fe_2Se_2$ with $T_c \sim 43$ K and neutral anti-PbO-type spacer layers, synthesized by the hydrothermal method. As shown in Fig. 1(a), the structure of $LiFeO_2Fe_2Se_2$ is constructed by alternately stacking the FeSe and $LiFeO_2$ layers. The $LiFeO_2$ is an anti-PbO-type spacer layer and has a cation-disordered cubic rocksalt structure (so-called α-$LiFeO_2$),[22] which is different in structure from the PbO-type *Ln*O layers in *Ln*OFeAs. In $LiFeO_2$ layers, Li and Fe randomly occupy half by half of the same site, which makes the $LiFeO_2$ layers electrically neutral. Generally speaking, the charge neutral nature of both FeSe and $LiFeO_2$ layers stops the charge transfer between them, which makes $LiFeO_2Fe_2Se_2$ strikingly different from other heavily electron-doped FeSe-derived superconductors.

Polycrystalline samples of $LiFeO_2Fe_2Se_2$ were prepared by the hydrothermal reaction method. 0.012–0.02 mol selenourea (Alfa Aesar, 99.97% purity), 0.0075 mol Fe powder (Aladdin Industrial, Analytical reagent purity), and 12 g LiOH H_2O (Sinopharm Chemical Reagent, A.R. purity) were put into a Teflon-lined steel autoclave (50 mL) and mixed together with 10 ml de-ionized water. The Teflon-lined autoclave was then tightly sealed and heated at 160 °C for 3–10 days. The polycrystalline samples acquired from the reaction system were shiny lamellar, which were then washed repeatedly with de-ionized water and dried at room temperature. The atomic ratio of Li:Fe:Se was determined to be 1.0:3.0:2.0 by inductively coupled plasma-atomic emission spectroscopy (ICP-AES), with an instrument error of 10%.

In order to get rid of the residua and to measure the transport properties, the as-synthesized polycrystalline samples were pressed into pellets and annealed at temperatures from 120 to

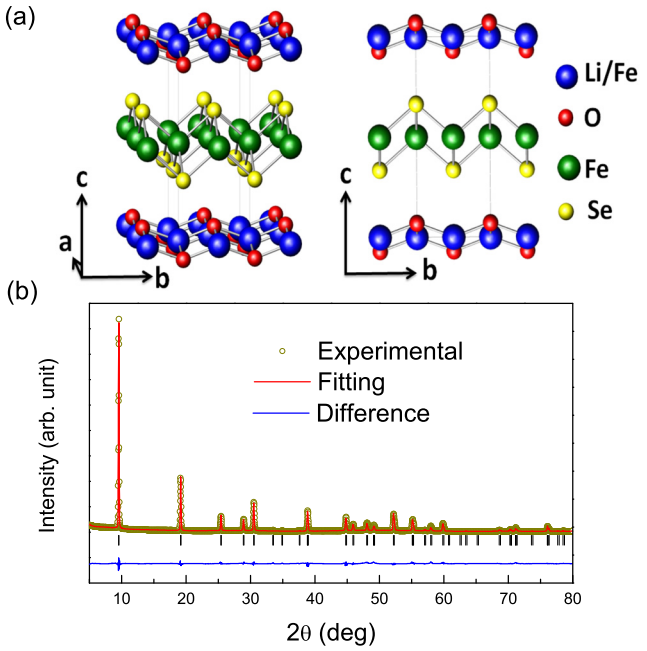

FIG. 1. (Color online) (a) A schematic view of the structure of $LiFeO_2Fe_2Se_2$. The layered structure consists of alternately stacking anti-PbO-type FeSe layers and $LiFeO_2$ layers. (b) XRD patterns together with Rietveld refinement results. The observed diffraction intensities are represented by yellow-green open circles, and the fitting results by the red solid line. The blue curve at the bottom is the difference between observed and fitting intensities. Short black vertical bars below the XRD patterns indicate the positions of allowed Bragg reflections.

200 °C for 5 h with an applied high pressure from 2 to 5 GPa. X-ray diffraction (XRD) was performed using an x-ray diffractometer (SmartLab-9, Rikagu Corp.) with Cu$K\alpha$ radiation and a fixed graphite monochromator. The XRD patterns were collected in the 2-theta range of 5°–80° with a scanning rate of 0.1°/min at room temperature. The lattice parameters and the crystal structure were refined using the Rietveld method in the program GSAS package, and Thompson-Cox-Hastings functions with asymmetry corrections were applied as reflection profiles. The magnetization measurements were carried out by a superconducting quantum interference device magnetic property measurement system (SQUID MPMS) (Quantum Design). To measure the magnetizations under pressure, we put the sample in a Teflon cell (EasyLab) with Daphne oil 7373 as the pressure media, and then placed the Teflon cell in a copper-beryllium pressure cell (EasyLab) and incorporated the pressure cell into the SQUID MPMS. The contribution of background magnetization to the sample at 2 K was less than 5%. The resistivity measurements were performed using a Quantum Design physical property measurement system (PPMS-9) and the corresponding results are shown in Fig. S1 of the Supplemental Material.[23]

Figure 1(b) shows the x-ray diffraction (XRD) pattern of the as-synthesized $LiFeO_2Fe_2Se_2$ taken at room temperature. The refinement fitting of the Rietveld analysis[24] was carried out with the structural model shown in Fig. 1(a), with alternately stacking of the anti-PbO-type FeSe and anti-PbO-type $LiFeO_2$ layers. All Bragg peaks of the product can be well indexed by a tetragonal structure with space group $P4/nmm$ (No. 129). The refinement pattern is shown in Fig. 1(b), and the crystallographic parameters from the refinement are listed in Table I. The obtained lattice constants of the tetragonal $LiFeO_2Fe_2Se_2$ are $a = 3.7926(1)$ Å and $c = 9.2845(1)$ Å, which has a much smaller a axis and larger c-axis lattice parameters than those of LnOFeAs (for instance, $a = 4.0337$ Å, $c = 8.7411$ Å for LaOFeAs),[25] respectively. The final R factors are fairly small ($R_{wp} = 0.0937$), which is evidence for the validity of the structural model we adopted. The unique bond distance of Fe-Se is 2.4347(1) Å and of Li(Fe)-O it is 2.0246(1) Å. The rather large distance, 3.6028(1) Å, between Se and O suggests that there are likely no chemical bonds (van der Waals gap) between neighboring FeSe and $LiFeO_2$ layers.

TABLE I. The crystallographic parameters from the Rietveld refinements of XRD data of $LiFeO_2Fe_2Se_2$. Space group: $P4/nmm$ (No. 129); $a = b = 3.7926(1)$ Å, $c = 9.2845(1)$ Å, $V = 133.54(1)$ Å^3, $R_{wp} = 0.0937$, $R = 0.0656$, $\chi^2 = 1.43$. g is the occupation factor.

Atom	x	y	z	g
Li	0.25	0.75	0	0.5
Fe1	0.25	0.75	0	0.5
Fe2	0.75	0.25	0.5	1
O	0.25	0.25	−0.0764(1)	1
Se	0.25	0.25	0.3355(1)	1
Bond length (Å)				
Fe2-Se	2.4347(1)× 4			
Fe2-Fe	2.6818(1)× 4			
Bond angle (deg)				
Se^{top}-Fe2-Se^{top}	102.31(1)× 2			
Se^{top}-Fe2-Se^{bottom}	113.16(1)× 4			

The magnetic susceptibility (χ) as a function of temperature for $LiFeO_2Fe_2Se_2$ is plotted in Fig. 2. The measurements were performed under an external field of $H = 10$ Oe. The as-synthesized sample shows a round diamagnetic transition around 40 K (see the inset), which is higher than $T_c \sim 37$ K observed in FeSe under pressure,[26] and a considerable shielding fraction of 44% at 5 K in the zero-field-cooling process. Such a large diamagnetism indicates that the as-synthesized $LiFeO_2Fe_2Se_2$ sample undergoes a bulk superconducting transition at around 40 K.

In the low-temperature solution synthetic route, the small sizes of the crystalline grains in the product can reduce the superconducting shielding fraction. To further enhance the sample quality, we applied a high-pressure annealing technique to get rid of the residual solution. The $LiFeO_2Fe_2Se_2$ sample was annealed under a high pressure of 5 GPa at $T = 150$ °C for 5 h, and its magnetic susceptibility is shown in Fig. 2(b). The sharp drop of χ at ∼43 K suggests that the high-pressure annealing procedure effectively enhanced the superconducting transition temperature T_c. The temperature-dependent electrical resistance of the annealed $LiFeO_2Fe_2Se_2$ sample is also measured, as shown in Fig. S1 of the Supplemental Material,[23] which shows a clear drop starting at 42 K in zero field, almost the same as the T_c inferred from the measurements of magnetic susceptibility. Zero resistance was achieved at around 20 K. The quite

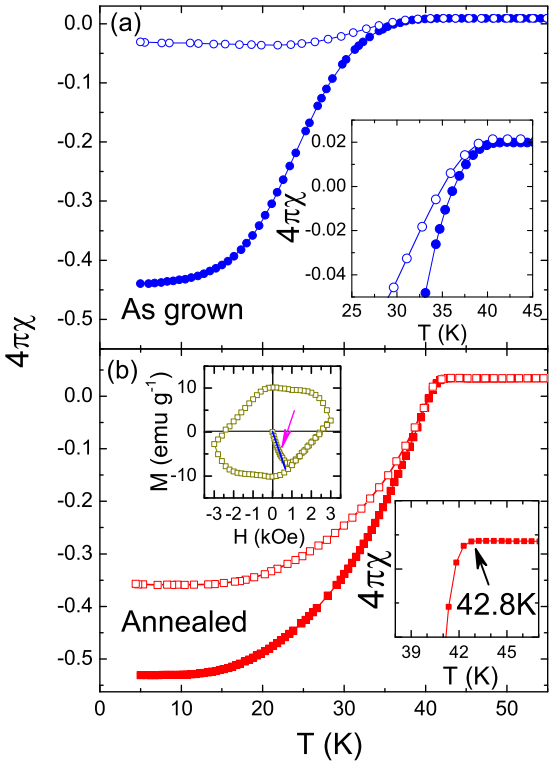

FIG. 2. (Color online) (a) The magnetic susceptibility of the as-synthesized $LiFeO_2Fe_2Se_2$ sample from the hydrothermal method. (b) The magnetic susceptibility of the sample after annealing under a high pressure of 5 GPa at $T = 150\,^{\circ}$C for 5 h. Solid symbols: Zero-field cooling (ZFC); open symbols: field cooling (FC). These data were collected under a magnetic field of 10 Oe. The inset in (a) is the zoom-in view around the superconducting transition of the as-synthesized sample. The bottom inset of (b) is the zoom-in view for ZFC data around the superconducting transition of the annealed sample, which indicates $T_c \sim 43$ K. The top inset of (b) is the M-H loop taken at 5 K for the annealed sample, where a linear H dependence of M with a negative slope can be recognized below 300 Oe in the low-field range (as the magenta arrow indicates).

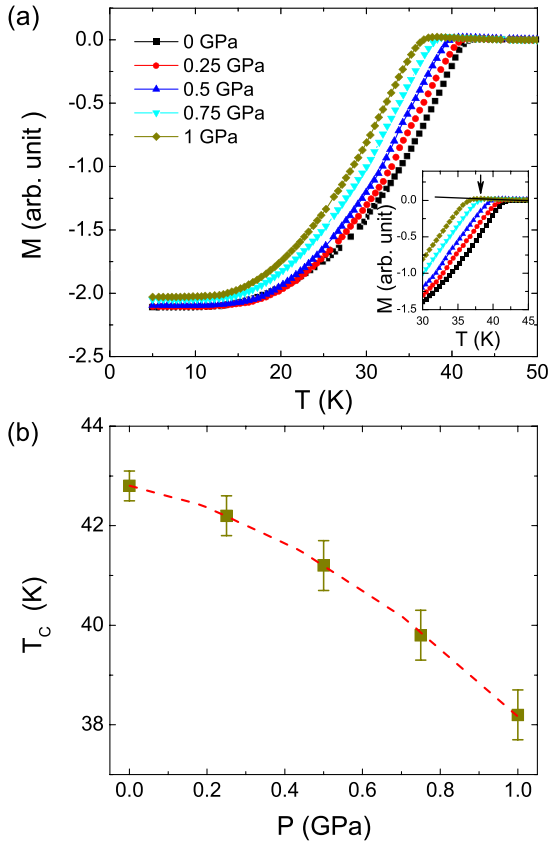

FIG. 3. (Color online) (a) The magnetizations (M) taken under various external pressures with $H = 10$ Oe in the ZFC mode. Before the measurement, the $LiFeO_2Fe_2Se_2$ sample was annealed under a high pressure of 5 GPa at $T = 150\,^{\circ}$C for 5 h. The inset shows the zoom-in view around the superconducting transitions. The arrow shows the beginning of the drop of M at 1 GPa, which represents the way to define T_c as shown in (b). (b) Pressure dependence of the superconducting transition temperatures T_c.

broad superconducting transition width (more than 20 K) arises from the weak links between the grains, consistent with the negative slope of the normal-state resistance. With an applied magnetic field of 7 T, the temperature where resistance starts to drop was suppressed to 34 K and the transition became rounder. Our data in Fig. 2 also indicate that the annealing procedure improved the diamagnetism. In the zero-field-cooling process, the χ of the annealed sample shows a superconducting shielding fraction of 53% at 5 K. More significantly, the χ in the field-cooling process reaches 36% of the theoretical value of perfect diamagnetism at 5 K, which is more than ten times larger than the value in the as-synthesized sample. The M-H loop in the inset, taken at 5 K, indicates that $LiFeO_2Fe_2Se_2$ is a type-II superconductor. A linear-H dependence of diamagnetic susceptibility with a negative slope can be observed in the low-field range below $\sim$300 Oe, which further confirms that the steep decrease of χ originates from the superconducting transition, and suggests a lower critical field $H_{c1} \approx 300$ Oe at 5 K.

Figure 3(a) presents the magnetization of annealed $LiFeO_2Fe_2Se_2$ under various pressures with $H = 10$ Oe in the zero-field-cooling process, and Fig. 3(b) summarizes the pressure dependence of T_c. The T_c monotonically decreases with increasing external pressure, indicating the suppression effect of pressure on superconductivity in $LiFeO_2Fe_2Se_2$. As the external pressure increases from 0 to 1 GPa, T_c decreases by $\sim$5 K with a negative slope $d[T_c/T_c(0)]/dP \sim -0.12$ GPa^{-1}. This value is larger than that observed in $K_xFe_{2-y}Se_2$ single crystals.[30] The difference can be attributed to the much larger height of the anion from the Fe layer (h) in $LiFeO_2Fe_2Se_2$ (1.527 Å, inferred from the refined parameters in Table I) than that in $K_xFe_{2-y}Se_2$ (1.459 Å, calculated from the crystallographic data in Ref. 12). As will be discussed later, the T_c is closely related to the chalcogen height, which can be easily suppressed by external pressure.[27]

In the FeAs-derived superconductors, T_c is found to be closely correlated to the anion height (h) from the Fe plane within the FePn (Pn = As, P) layer.[28] As shown in Fig. 1 of Ref. 28, T_c reaches a maximum at $h_0 \approx 1.38$ Å and decreases rapidly with a deviation of h from h_0. We can also examine this correlation for FeSe-derived compounds. In Fig. 4, we plot T_c

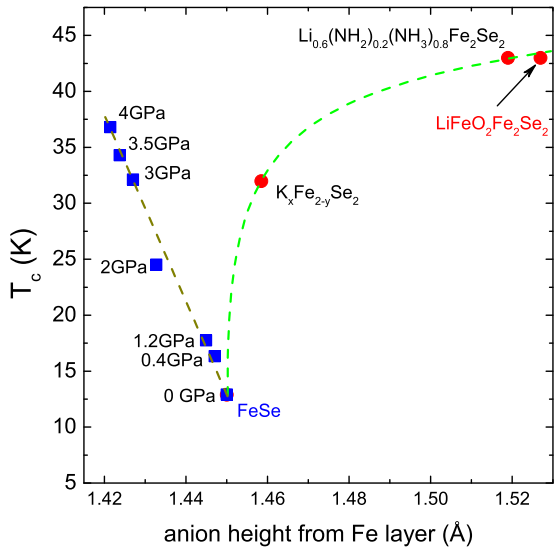

FIG. 4. (Color online) T_c vs chalcogen (Se) height for the FeSe-derived superconductors. The data for FeSe under high pressure are from Ref. 29, indicated by blue solid squares. Red solid circles are the data of the intercalated FeSe superconductors from Ref. 12 ($K_xFe_{2-y}Se_2$), Ref. 16 [$Li_{0.6}(NH_2)_{0.2}(NH_3)_{0.8}Fe_2Se_2$], and the present work.

as a function of chalcogen (Se) height from the Fe layer for FeSe-derived superconductors, which shows that the T_c is also related to the anion height in iron selenide superconductors. It is evident that T_c monotonically increases when the anion height from the Fe layer deviates from 1.45 Å to a lower or a higher value. Such a V-shaped h dependence of T_c in FeSe-derived superconductors is in sharp contrast to the inverse V-shaped one in FeAs-based superconductors. In $LiFeO_2Fe_2Se_2$, the anion height is 1.527 Å, which is much larger than the value of 1.45 Å in FeSe.[29] By applying external pressure, the value of the anion height can be reduced, and according to the plot in Fig. 4, T_c should decrease. Indeed, this is what we have observed in $LiFeO_2Fe_2Se_2$, as shown in Fig. 3(b). A similar pressure dependence of T_c has been observed also in $K_xFe_{2-y}Se_2$,[27,30] which is consistent with the general trend for compounds with a large anion height shown in Fig. 4.

Both the $LiFeO_2$ and FeSe layers in $LiFeO_2Fe_2Se_2$ are electrically neutral, so the $LiFeO_2$ layers do not act as electron donors, while other FeSe-derived superconductors with a Se height larger than 1.45 Å are heavily electron doped. In this regard, changing the carrier concentration by the ratio of Li/Fe can probably control T_c or achieve a higher T_c in $LiFeO_2Fe_2Se_2$. In addition, it is reported that the extension of the lattice in the ab plane can lead to an increase of T_c.[31] Thus, it is possible to increase T_c by adjusting the anion height or lattice constants of the ab plane with different spacer layers in FeSe-derived superconductors. On the other hand, as reported in Ref. 32, α-$LiFeO_2$ shows antiferromagnetism with a large effective moment of $4.53(3)\mu_B$ and a Weiss constant of $-186(3)$ K, and the magnetic transition temperature is dependent on the degree of cation ordering. Since the spin degree of freedom plays an important role in iron-based high-T_c superconductors,[33] it is quite significant to study the effect of magnetism in the $LiFeO_2$ layer on the FeSe layer to understand high-T_c superconductivity.

In the present work, we have synthesized a FeSe-based layered material $LiFeO_2Fe_2Se_2$ through the hydrothermal reaction method, in which an anti-PbO-type $LiFeO_2$ spacer layer was intercalated between FeSe layers. The superconductivity therein can reach as high as 43 K, which is much higher than 8 K in β-FeSe. This work expands the categories of iron-based superconductors and opens a window to achieve higher T_c in iron-based superconductors.

The authors are grateful for discussions with Z. Sun and T. Wu, and help with manuscript preparation by Z. Sun. This work is supported by the National Natural Science Foundation of China (Grants No. 11190021, No. 51125006, and No. 91122034), the "Strategic Priority Research Program (B)" of the Chinese Academy of Sciences (Grant No. XDB04040100), and the National Basic Research Program of China (973 Program, Grant No. 2011CBA00101).

*Corresponding author: huangfq@mail.sic.ac.cn
†Corresponding author: chenxh@ustc.edu.cn

[1] Y. Kamihara, T. Watanabe, M. Hirano, and H. Hosono, J. Am. Chem. Soc. **130**, 3296 (2008).
[2] X. H. Chen, T. Wu, G. Wu, R. H. Liu, H. Chen, and D. F. Fang, Nature (London) **453**, 761 (2008).
[3] M. Rotter, M. Tegel, and D. Johrendt, Phys. Rev. Lett. **101**, 107006 (2008).
[4] K. Sasmal, B. Lv, B. Lorenz, A. M. Guloy, F. Chen, Y.-Y. Xue, and C.-W. Chu, Phys. Rev. Lett. **101**, 107007 (2008).
[5] X. C. Wang, Q. Q. Liu, Y. X. Lv, W. B. Gao, L. X. Yang, R. C. Yu, F. Y. Li, and C. Q. Jin, Solid State Commun. **148**, 538 (2008).
[6] P. M. Shirage, K. Kihou, C. H. Lee, H. Kito, H. Eisaki, and A. Lyo, Appl. Phys. Lett. **97**, 172506 (2010).
[7] P. M. Shirage, K. Kihou, C. H. Lee, H. Kito, H. Eisaki, and A. Lyo, J. Am. Chem. Soc. **133**, 9630 (2011).
[8] D. R. Parker, M. J. Pitcher, P. J. Baker, I. Franke, T. Lancaster, S. J. Blundell, and S. J. Clarke, Chem. Commun. **2009**, 2189 (2009).
[9] Z. A. Ren, G. C. Che, X. L. Dong, J. Yang, W. Lu, W. Yi, X. L. Shen, Z. C. Li, L. L. Sun, F. Zhou, and Z. X. Zhao, Europhys. Lett. **83**, 17002 (2008).
[10] Z. A. Ren, W. Lu, J. Yang, W. Yi, X. L. Shen, Z. C. Li, G. C. Che, X. L. Dong, L. L. Sun, F. Zhou, and Z. X. Zhao, Chin. Phys. Lett. **25**, 2215 (2008).
[11] F. C. Hsu, J. Y. Luo, K. W. Yeh, T. K. Chen, T. W. Huang, P. M. Wu, Y. Y. Lee, Y. L. Huang, Y. Y. Chu, D. C. Yan, and M. K. Wu, Proc. Natl. Acad. Sci. USA **105**, 14262 (2008).
[12] J. Guo, S. Jin, G. Wang, S. Wang, K. Zhu, T. Zhou, M. He, and X. Chen, Phys. Rev. B **82**, 180520(R) (2010).
[13] M. H. H. D. Wang, C. H. Dong, Z. J. Li, C. M. Feng, J. Chen, and H. Q. Yuan, Europhys. Lett. **94**, 27009 (2011).

[14] A. F. Wang, J. J. Ying, Y. J. Yan, R. H. Liu, X. G. Luo, Z. Y. Li, X. F. Wang, M. Zhang, G. J. Ye, P. Cheng, Z. J. Xiang, and X. H. Chen, Phys. Rev. B **83**, 060512(R) (2011).

[15] T. P. Ying, X. L. Chen, G. Wang, S. F. Jin, T. T. Zhou, X. F. Lai, H. Zhang, and W. Y. Wang, Sci. Rep. **2**, 426 (2012).

[16] M. Burrard-Lucas, D. G. Free, S. J. Sedlmaier, J. D. Wright, S. J. Cassidy, Y. Hara, A. J. Corkett, T. Lancaster, P. J. Baker, S. J. Blundell, and S. J. Clarke, Nat. Mater. **12**, 15 (2013).

[17] A. Krzton-Maziopa, E. V. Pomjakushina, V. Y. Pomjakushin, F. von Rohr, A. Schilling, and K. Conder, J. Phys.: Condens. Matter **24**, 382202 (2012).

[18] E.-W. Scheidt, V. R. Hathwar, D. Schmitz, A. Dunbar, W. Scherer, F. Mayr, V. Tsurkan, J. Deisenhofer, and A. Loidl, Eur. Phys. J. B **85**, 279 (2012).

[19] W. Li, H. Ding, P. Deng, K. Chang, C. Song, K. He, L. Wang, X. Ma, J.-P. Hu, X. Chen, and Q.-K. Xue, Nat. Phys. **8**, 126 (2012).

[20] W. Bao, Q. Z. Huang, G. F. Chen, M. A. Green, D. M. Wang, J. B. He, and Y. M. Qiu, Chin. Phys. Lett. **28**, 086104 (2011).

[21] W. Bao, G. N. Li, Q. Z. Huang, G. F. Chen, J. B. He, D. M. Wang, M. A. Green, Y. M. Qiu, J. L. Luo, and M. M. Wu, Chin. Phys. Lett. **30**, 027402 (2013).

[22] T. Shirane, R. Kanno, Y. Kawamoto, Y. Takeda, M. Takano, T. Kamiyama, and F. Izumi, Solid State Ionics **79**, 227 (1995).

[23] See Supplemental Material at http://link.aps.org/supplemental/10.1103/PhysRevB.89.020507 for results of the resistance measurements on the annealed sample, degradation of superconductivity at room temperature in an inert atmosphere, and the decomposition at high temperature for the $LiFeO_2Fe_2Se_2$ sample.

[24] A. C. Larson and R. B. Von Dreele, Los Alamos National Laboratory Report No. LAUR 86-748, 1994 (unpublished).

[25] T. Nomura, S. W. Kim, Y. Kamihara, M. Hirano, P. V. Sushko, K. Kato, M. Takata, A. L. Shluger, and H. Hosono, Supercond. Sci. Technol. **21**, 125028 (2008).

[26] S. Medvedev, T. M. McQueen, I. A. Troyan, T. Palasyuk, M. I. Eremets, R. J. Cava, S. Naghavi, F. Casper, V. Ksenofontov, G. Wortmann, and C. Felser, Nat. Mater. **8**, 630 (2009).

[27] L. L. Sun, X. J. Chen, J. Guo, P. W. Gao, Q. Z. Huang, H. D. Wang, M. H. Fang, X. L. Chen, G. F. Chen, Q. Wu, C. Zhang, D. C. Gu, X. L. Dong, L. Wang, K. Yang, A. G. Li, X. Dai, H. K. Mao, and Z. X. Zhao, Nature (London) **483**, 67 (2012).

[28] Y. Mizuguchi, Y. Hara, K. Deguchi, S. Tsuda, T. Yamaguchi, K. Takeda, H. Kotegawa, H. Tou, and Y. Takano, Supercond. Sci. Technol. **23**, 054013 (2010).

[29] S. Margadonna, Y. Takabayashi, Y. Ohishi, Y. Mizuguchi, Y. Takano, T. Kagayama, T. Nakagawa, M. Takata, and K. Prassides, Phys. Rev. B **80**, 064506 (2009).

[30] J. J. Ying, X. F. Wang, X. G. Luo, Z. Y. Li, Y. J. Yan, M. Zhang, A. F. Wang, P. Cheng, G. J. Ye, Z. J. Xiang, R. H. Liu, and X. H. Chen, New J. Phys. **13**, 033008 (2011).

[31] S. Y. Tan, Y. Zhang, M. Xia, Z. R. Ye, F. Chen, X. Xie, R. Peng, D. F. Xu, Q. Fan, H. C. Xu, J. Jiang, T. Zhang, X. C. Lai, T. Xiang, J. P. Hu, B. P. Xie, and D. L. Feng, Nat. Mater. **12**, 634 (2013).

[32] M. Tabuchi, S. Tsutsui, C. Masquelier, R. Kanno, K. Ado, I. Matsubara, S. Nasu, and H. Kageyama, J. Solid State Chem. **140**, 159 (1998).

[33] G. R. Stewart, Rev. Mod. Phys. **83**, 1589 (2011).